Observation of Second-Harmonic Ion Bernstein Waves Excited by Fast-Wave Mode Conversion in the Microtor Tokamak

H. Park, N. C. Luhmann, Jr., W. A. Peebles, and R. Kirkwood
University of California, Los Angeles, California 90024
(Received 20 December 1983)

This paper reports the first conclusive observation of ion Bernstein waves near the second-harmonic cyclotron layer in a single-ion-species tokamak plasma. The interpretation that the ion Bernstein waves are generated through fast-wave mode conversion at the second-harmonic cyclotron layer is supported by wave dispersion measurements as well as the observation of the long-wavelength fast wave by laser scattering techniques.

PACS numbers: 52.35.Fp, 52.50.Gj

In recent years, heating in the ion cyclotron range of frequencies (ICRF) has been under active study as an efficient source of supplementary heating in tokamak plasmas.[1-5] At the University of California at Los Angeles (UCLA), far-infrared (FIR) collective Thomson scattering has been employed to probe directly and identify the various plasma waves excited. This has served to improve the understanding of ICRF wave physics while also offering potential diagnostic applications.[6,7]

Previous FIR scattering studies of ICRF waves in the Microtor plasma at UCLA identified ion Bernstein waves generated via mode conversion at the ion-ion hybrid layer in a mixed-ion-species plasma.[6,8] The present paper reports the conclusive identification of ion Bernstein waves excited at the *second-harmonic* cyclotron layer in a *pure hydrogen* plasma. In addition, a long-wavelength mode, identified as the fast magnetosonic wave, has been directly probed internally for the first time by use of collective Thomson scattering techniques. Observations strongly support the interpretation that fast-wave mode conversion at the second-harmonic cyclotron layer is responsible for the ion Bernstein wave generation.

The experiments were performed in the UCLA Microtor tokamak. The device parameters are as follows: major radius, $R_0 = 40$ cm; minor radius, 12.5 cm; $B_T = 10$–25 kG; $I_T = 60$–100 kA; $n_e = 10^{13} - 10^{14}$ cm^{-3}; $T_e \leq 600$ eV; and $T_i \leq 300$ eV. The ICRF antenna was located toroidally at a reference plane of 45° whereas the FIR scattering system was located at 0°. Quarter-turn electromagnetic antennas (10 MHz $\leq \omega/2\pi \leq 40$ MHz, $P_{\rm rf} \leq 25$ kW) located in the low-field plasma region were primarily utilized, although electrostatic antennas were also used occasionally to confirm experimental observations.

The far-infrared–laser scattering system employed for these measurements is described in detail by Peebles *et al.*[9] The radiation source is a cw optically pumped $^{13}CH_3F$ laser operating at 1222 μm (245 GHz) and producing ≈ 10 mW output power. The output power radiation is divided via a mesh beam splitter into a local oscillator (LO) beam and probe beam. The local oscillator beam provides rf drive for a quasioptical Schottky-diode mixer. The frequency-shifted scattered radiation is collected at a particular scattering angle (0°–20°) and then combined with the LO beam in the mixer to produce a signal at the plasma wave frequency. The scattered electric field amplitude is monitored with use of a tunable narrow-band filter and is given by

$$E_s(\theta_s, k_w) \propto \tilde{n} \exp[-\tfrac{1}{2}(k_w - 2k_0 \sin\tfrac{1}{2}\theta_s)^2 a_0^2], \quad (1)$$

where $\tilde{n}$ is the density fluctuation amplitude, k_0 is the incident far-infrared–laser wave number, θ_s is the scattering angle, a_0 is the beam waist in the scattering volume, and k_w is the density fluctuation wave number.

The Gaussian term is simply the result of wave-number matching. When the scattering wave number $[k_s = 2k_0 \sin(\theta_s/2)]$ matches k_w, this term is a maximum. If k_w changes so that a mismatch occurs, the scattered electric field falls off as a Gaussian with an e^{-1} width determined by the beam waist. The output of the laser was weakly focused to a beam waist of ≈ 1.8 cm on the equatorial plane of the plasma, resulting in a wave-number resolution $\Delta k = \pm 1$ cm^{-1}. Variation of the scattering angle allowed wave numbers k_w in the range $0 < k_w < 18$ cm^{-1} to be observed. The spatial resolution along the incident beam is dependent on the scattering angle. However, in Microtor the majority of the scattering data were obtained for $\theta_s \leq 10°$ and were essentially chord averaged.

The scattered electric field for $k = 7.2$ cm^{-1} at a minor radius of 6 cm is illustrated in Fig. 1 together

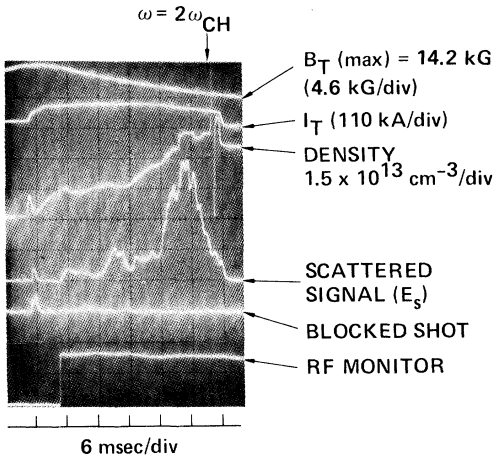

FIG. 1. The time development of the scattered electric field ($k = 7.2$ cm^{-1}) illustrated together with plasma current, toroidal magnetic field, electron density, and rf monitor. The signal is chord averaged at a major radius of 46 cm and the rf frequency is 25 MHz. The temporal variation of the toroidal field locates the second-harmonic cyclotron layer at one instant of time, as indicated by the arrow. The maximum central toroidal field is 14.2 kG.

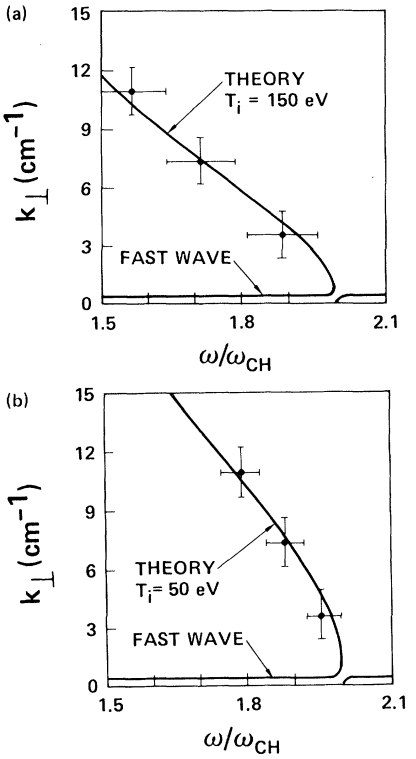

FIG. 2. (a) The experimentally measured wave dispersion for chord-averaged data at a major radius of 44 cm. The solid line represents a theoretical fit using a full electromagnetic code ($k_\parallel = 0.07$ cm^{-1}, $n_e = 3.8 \times 10^{13}$ cm^{-3}, $B_T = 8.7$ kG, $f_{rf} = 26.2$ MHz, $T_i = 150$ eV, $T_e = 400$ eV). (b) The experimental dispersion at a major radius of 48 cm. The full electromagnetic code uses the following parameters: $k_\parallel = 0.07$ cm^{-1}, $n_e = 1.6 \times 10^{13}$ cm^{-3}, $B_T = 8.7$ kG, $f_{rf} = 26.2$ MHz, $T_i = 50$ eV, $T_e = 150$ eV.

with plasma current, toroidal magnetic field, electron density, and rf monitor. The rf frequency was 25 MHz and the maximum toroidal field at the plasma center was 14.2 kG. Operation in a pure hydrogen plasma at the second-harmonic ion cyclotron frequency eliminates the possibility of overlap with any other fundamental cyclotron resonance. The only remaining coincidences occur at higher harmonics (e.g., fourth harmonic of deuterium) whose effects should be negligible.[1] The location in time of the second-harmonic cyclotron frequency (at $R = 46$ cm) resulting from the temporal variation of B_T is indicated by the arrow. The trace with the probe beam blocked indicates the background level of synchrotron emission and electromagnetic interference. The signal-to-noise level is seen to be excellent even though input rf powers of $\lesssim 15$ kW were typical.

Experimentally, the wave dispersion can be determined by performing an angular scan. The peak in the scattered signal [Eq. (1)] occurs when the scattering wave number, k_s, matches the density fluctuation wave number, k_w. This instant in time corresponds to a particular value of ω/ω_{ch} determined by the spatial and temporal variation of the toroidal field, thereby allowing the dispersion to be determined.

Figures 2(a) and 2(b) illustrate the measured dispersion for chord-averaged data centered at major radii of 44 and 48 cm. The solid lines represent the best theoretical fit to the experimental data. A full electromagnetic code was used to solve the hot-plasma dispersion equation in the local approximation. Electromagnetic modifications to purely electrostatic solutions of the ion Bernstein wave dispersion were found to be nonnegligible, improving agreement between theory and experiment especially at small wave number. Figure 2 clearly illustrates that the measured dispersion is very sensitive to ion-temperature variations and agrees well with a theoretical model based on fast-wave mode conversion to ion Bernstein waves at the second-harmonic cyclotron layer. It should be noted that the slope of the dispersion is relatively insensitive to variations in electron density, electron temperature, and parallel wave number. Extrapolation of the experimental measurements suggests a central-chord–averaged ion temperature of ≈ 200 eV

which is somewhat lower than that measured by a charge-exchange analyzer (≈ 280 eV, Lee[10]). This discrepancy may be a result of the exact nature of the spatial-averaging processes involved but clearly warrants further investigation.

The interpretation that the observed waves are ion Bernstein waves generated through mode conversion at the second-harmonic cyclotron layer is based on a number of observations. First, as described above, the experimentally measured dispersion agrees well with theory. The waves exist close to, but below, the second-harmonic ion cyclotron frequency and the measured dispersion displays the expected ion-temperature dependence. Second, the waves are only observed when magnetic induction excitation was adopted; purely electrostatic excitation (by use of a poloidal metallic plate whose potential was varied) failed to generate any observable waves close to the second-harmonic cyclotron frequency. Finally, observation of a long-wavelength ($k < 1$ cm^{-1}) mode, identified with the fast magnetosonic wave, further supports the mode-conversion interpretation.

This long-wavelength mode has been observed with use of the FIR scattering system. A typical chord-averaged scattering signal at $R = 34$ cm is illustrated in Fig. 3 for an rf frequency of 36 MHz. The following characteristics should be noted. First, scattering signals were only observed at very small scattering angles within the k resolution of the scattering system (i.e., $k \lesssim 1$ cm^{-1}). In this situation, both perpendicular and parallel wave numbers are probed simultaneously. Second, the signals were observed over a wide range of frequency ($1.1 \lesssim \omega/\omega_{ch} \lesssim 2.9$). In Fig. 3, for example, the time-varying toroidal field sweeps out a range of ω/ω_{ch} from 1.7 to 2.9. This is in strong contrast to the short-wavelength ion Bernstein wave which exists close to the second-harmonic ion cyclotron layer and has not been observed at higher frequencies. The above observations result in a measured dispersion in reasonable agreement with that illustrated in Fig. 2 for the fast magnetosonic wave. However, scattering measurements, at present, can only set an upper limit on the fast-wave perpendicular wave number ($k \lesssim 1$ cm^{-1}). In the future, far-forward scattering measurements may permit a more accurate determination of both perpendicular and parallel wavelength.[11]

In addition to the above spectral observations, it should also be noted that the scattering signals correlated well with magnetic probes, as illustrated in Fig. 3. Strong modulation of the scattered signal, characteristic of eigenmode structure, was also observed, as expected for weakly damped fast waves. Note that the scattering system is sensitive to the electrostatic component in the wave (i.e., $\tilde{n}$) whereas the magnetic probe detects only magnetic field. In addition, the magnetic probe represents a local measurement in the plasma edge ($R = 30$ cm) whereas the scattering signal is chord averaged at $R = 34$ cm. It is not surprising, therefore, that, although the correlation is good, the details are not exact. Finally, detailed Langmuir-probe measurements in a low-density, low-temperature plasma ($n_e \approx 3 \times 10^{11}$ cm^{-3}, $T_e \approx 5$ eV) using the identical electromagnetic antenna have permitted determination of $k_{\parallel}$ and $k_{\perp}$, while also allowing cutoffs to be clearly displayed. Agreement between experiment and theory for the fast magnetosonic wave was excellent.[12] The accumulated evidence presented strongly confirms our initial interpretation that the long-wavelength mode observed in tokamak discharges is, in fact, the fast magnetosonic wave.

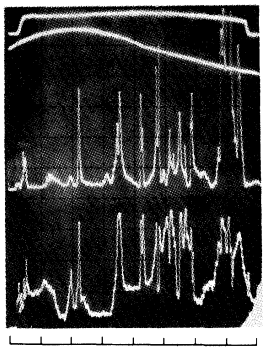

FIG. 3. The scattered electric field from the long-wavelength mode ($k < 1$ cm^{-1}) illustrated together with magnetic probe, plasma current and toroidal magnetic field signals. The scattered signal was chord averaged at a major radius of 34 cm whereas the magnetic probe was located in the edge plasma at a major radius of ≈ 30 cm. The rf frequency in this instance was 36 MHz. The toroidal-field temporal variation results in a sweep of ω/ω_{ch} from 1.7 to 2.9.

In summary, excitation of ion Bernstein waves close to the second-harmonic cyclotron frequency in a pure hydrogen plasma has been observed in the UCLA Microtor tokamak plasma. The interpretation that the generation mechanism is fast-magnetosonic-wave mode conversion is supported by a number of experimental observations. These include good agreement between the experimentally determined and theoretically predicted ion Bernstein wave dispersion together with observation of the long-wavelength fast magnetosonic wave.

The authors wish to thank Dr. R. J. Taylor for many illuminating discussions as well as the strong support provided by Z. Lucky and the UCLA tokamak technical staff. This work was supported by the U. S. Department of Energy, Office of Fusion Energy under Contract No. DE-AM03-76SF00010, P.A. No. DE-AT03-76ET53019, TaskIIIA.

[1]D. Q. Hwang, J. Hosea, H. Thompson, J. R. Wilson, S. Davis, D. Herndon, R. Kaita, D. Mueller, S. Suckewer, C. Daughney, and P. Colestock, Phys. Rev. Lett. **51**, 1865 (1983).

[2]D. Hwang *et al.*, in *Proceedings of the Ninth International Conference on Plasma Physics and Controlled Nuclear Fusion Research, Baltimore, 1982* (International Atomic Energy Agency, Vienna, 1983), Vol. 2.

[3]Equipe TFR, in *Proceedings of the International Conference on Plasma Physics, Nagoya, 1980,* edited by K. Takayama (Fusion Research Association of Japan, Nagoya, 1980), Vol. 2, p. 226.

[4]TFR Group, A. Truc, and D. Gresillon, Nucl. Fusion **22**, 1577 (1982).

[5]M. Ono, K. L. Wong, and G. A. Wurden, Phys. Fluids **26**, 298 (1983).

[6]P. Lee, R. J. Taylor, W. A. Peebles, H. Park, C. X. Yu, Y. Xu, N. C. Luhmann, Jr., and S. X. Jin, Phys. Rev. Lett. **49**, 206 (1982).

[7]P. Lee, N. C. Luhmann, Jr., H. Park, W. A. Peebles, R. J. Taylor, Y. Xu, and C. X. Yu, in Proceedings of the Workshop on Sub-millimeter Diagnostic Techniques, Nagoya, January 1982 (unpublished), p. 60.

[8]D. Swanson, Phys. Fluids **18**, 1269 (1975).

[9]W. A. Peebles, N. C. Luhmann, Jr., A. Mase, H. Park, and A. Semet, Rev. Sci. Instrum. **52**, 360 (1981).

[10]P. Lee, private communication.

[11]D. E. Evans, M. von Hellerman, and E. Holzhauer, Plasma Phys. **24**, 819 (1982).

[12]H. Park, Ph.D. thesis, University of California at Los Angeles, 1984 (unpublished).

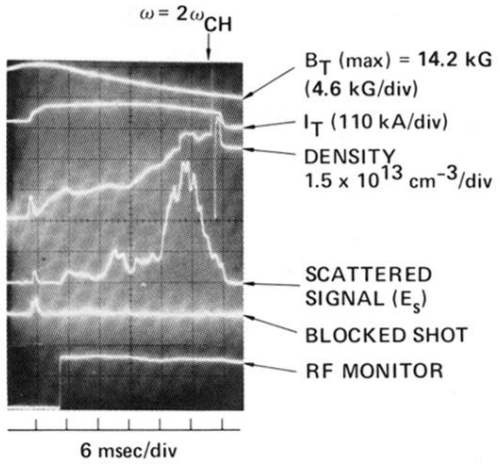

FIG. 1. The time development of the scattered electric field ($k = 7.2$ cm^{-1}) illustrated together with plasma current, toroidal magnetic field, electron density, and rf monitor. The signal is chord averaged at a major radius of 46 cm and the rf frequency is 25 MHz. The temporal variation of the toroidal field locates the second-harmonic cyclotron layer at one instant of time, as indicated by the arrow. The maximum central toroidal field is 14.2 kG.

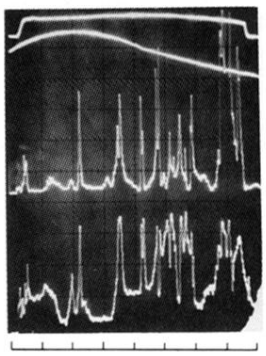

FIG. 3. The scattered electric field from the long-wavelength mode ($k < 1$ cm^{-1}) illustrated together with magnetic probe, plasma current and toroidal magnetic field signals. The scattered signal was chord averaged at a major radius of 34 cm whereas the magnetic probe was located in the edge plasma at a major radius of ≈ 30 cm. The rf frequency in this instance was 36 MHz. The toroidal-field temporal variation results in a sweep of ω/ω_{ch} from 1.7 to 2.9.